https://doi.org/10.1016/j.measurement.2019.107051

Uncertainty budget analysis for worm and worm gear single-flank rolling tests.

M. Pueo[1], R. Acero[2*], M.A. Lope[2], J. Santolaria[2,3]

[1] Centro Universitario de la Defensa. Academia General Militar. Ctra. Huesca s/n. 50090 Zaragoza, Spain.
[2] University of Zaragoza. Department of Design and Manufacturing Engineering, c/María de Luna 3, 50018 Zaragoza, Spain.
[3]Instituto de Investigación en Ingeniería de Aragón (I3A), 50018 Zaragoza, Spain.

*E-mail address: racero@unizar.es

Abstract
This work presents the development of a new uncertainty budget model for worm and worm gear single-flank rolling tests. Also known as tangential composite test, this functional test offers an alternative way to analytical measurements to verify the accuracy grade of a gear obtaining also geometric information. The lack of available standards for the evaluation and calibration of these test equipment generates repeatable testers but not comparable ones because of the lack of traceability in the test results. The authors identified in this paper the different error sources affecting the dynamic measuring process, weighting them with the corresponding experimentally quantified sensitivity factors. The global expanded uncertainty of *Fi'*, *fi'* and *Fp*' parameters was calculated for an industrial single flank rolling tester. This uncertainty budget served as a basis for defining an optimized model that minimizes the effects of the main error contributions in worm and worm gear single-flank rolling tests.

Keywords: transmission error; gear metrology**;** worm gear; tangential composite; single-flank

1 Introduction

Any type of measurement that is performed repeatedly under the same operating conditions, does not normally give identical results. Therefore, the validity of a measurement process involves estimating an expected range of values, known as measurement uncertainty, where the expected conventional true value is found. According to [1] the measurement uncertainty could be defined as a non-negative parameter characterizing the dispersion of the quantity values being attributed to a measurand. The GUM or guide to the expression of uncertainty in measurement [2] gives a framework for uncertainty analysis and estimation in measurement processes. The estimation of measurement uncertainty links with the calibration of the measuring instrument, which is a key part of the process. In addition, it is important to point out that there are more influences besides the instrument that could affect the measurement uncertainty, leading in this way to the concept of uncertainty of the complete measuring process. The evaluation of measurement uncertainty tries also to estimate in which way the different error sources affect the measuring process, whether individually or combined.

Gear metrology covers a broad range of measurement modalities depending on the type of information provided by the method [3–5], from traditional manual methods to high-precision gear-measuring instruments (GMIs) which offer similar levels of performance to CMMs [6]. Analytical measurements quantify the readings obtained in gear's production in order to evaluate the conformity of the gear in terms of geometric parameters. They are widely used for initial inspection purposes [7]. On the other side, functional tests also known as "rolling" tests, offer another way to verify the accuracy grade of a gear giving as a result parameters related to the operating conditions of the gear. In these tests, a rotated test gear is normally compared to a master gear of better tolerance. The results of these tests include the sum of various simultaneous influences [8–10] and allow establishing the accuracy grade of the gear and obtaining geometric information. Recent studies have been identified related to gear rolling tests, both radial and tangential composite [11–14]. This is why the estimation of rolling tests uncertainty is of paramount importance for understanding and optimizing the measurement process with this type of machines.

In general, the verification of gears implies the measurement of complex geometries normally affected by a large number of error sources. This often prevents the estimation of small uncertainties

[15]. In the particular case of gear rolling tests, this situation is aggravated by dynamic measurements. The mere fact of rolling a gear against a master is not a one-dimensional measurement, although the result does. Measurements are commonly evaluated in micrometres, range of dimension where any remaining material or dirt on the surface can distort the gear inspection. All of this, together with the lack of calibrated rolling gauges, make that determining the uncertainty of the measurement process is the most appropriate method to ensure the accuracy of these dynamic measurement systems [16,17].

ISO 18653: 2003 [18] proposes several methods to estimate the uncertainty of gear measurement. Each method differs considerably in complexity, implementation time and cost, so their choice depends on the application:

- The decomposition and substitution method applies in national and primary calibration facilities;

- The comparison method, used in the gear industry, verifies the behaviour of the measuring equipment;

- The uncertainty budget method following the guidelines of the GUM [2] is commonly used in secondary calibration laboratories or in industrial facilities that require a more accurate estimation of the capacity of the measurement process.

In accordance to ANSI/AGMA 2116-05 standard [19] these methods could be used to calculate the measurement uncertainty of double flank rolling tests (radial composite test). This standard proposes a general expression of the substitution method equation to be applied to double-flank rolling tests, maintaining the comparison method recommended in ISO 18653: 2003 [18]. On the contrary, there are neither specific regulations nor even guidelines, for estimating the measurement uncertainty of transmission errors in single-flank rolling machines (tangential composite). Despite the different measurement principles of both rolling tests, they have similar testing and evaluation procedures. Therefore, the methods established in [19] could be considered as adequate for the uncertainty estimation of single flank rolling test measurements.

Regarding the different error sources to be considered in the uncertainty budget for rolling test machines, ANSI / AGMA 2116-05 [19] includes a list of the main contributions to be taken into account. This list contains factors such as: the environment's influence, including temperature and vibrations; the calibration process and devices used; the repeatability and reproducibility of the instrument; the mechanical alignment of the components, the assembly errors and the eccentricity of the axes; the filtering system, the equipment's dynamic response and accuracy; the control system and execution of the tests; the evaluation of the measurement software; and finally the operator. In addition, ISO / TR 10064-5: 2005 [20] establishes that the most common problems that increase the measurement uncertainty are usually the inappropriate specifications; runout errors and eccentricities during the manufacture and measurement of the gear; assembly errors of the measuring instruments and machine tools; and inadequate measurement methods.

However, there are no studies showing the detailed identification procedure of error sources affecting to single flank rolling tests, being the uncertainty budget method the most appropriate for this purpose. This method would allow us to define the individual contribution of each error source in the testing and to implement corrective actions to increase the measurement accuracy. The available standards for verification and calibration of rolling testers such as [19] show no expression to apply the uncertainty budget method and they are mainly focus on double flank test type for gears with parallel axes. This fact also hinders its application to other types of gears' transmission. All of it allows considering the rolling testers as repeatable but not comparable because of the lack of traceability in the test results [14].

Based on these facts, this work presents the first uncertainty budget analysis for worm and worm gear single-flank rolling tests. On these grounds, we identify the different error sources affecting the measurement process following the guidelines of [19] and [20]. Their influences, which are included

as uncertainty components in the budget, are weighted with the application of experimentally quantified sensitivity coefficients. Finally, we develop the uncertainty budget model for single-flank rolling tests applying it to an industrial single-flank rolling test machine. A further optimization of the uncertainty budget obtained for the single-flank rolling machine is proposed in the final part of the paper.

2 Single-flank rolling test

In this work, we will focus on the single-flank or tangential composite test where a test gear is rotated against a master gear at their specified centre distance, subject to nominal geometric assembly conditions (*Fig. 1*). The test verifies the transmission error, comparing the rotational variation measured between the two gears. The low speed and a slightly braked spindle conditions in the test try to avoid the noise in the results due to dynamic influences. The tangential composite test could be also applied to paired gears to evaluate the transmission error during a complete revolution [10].

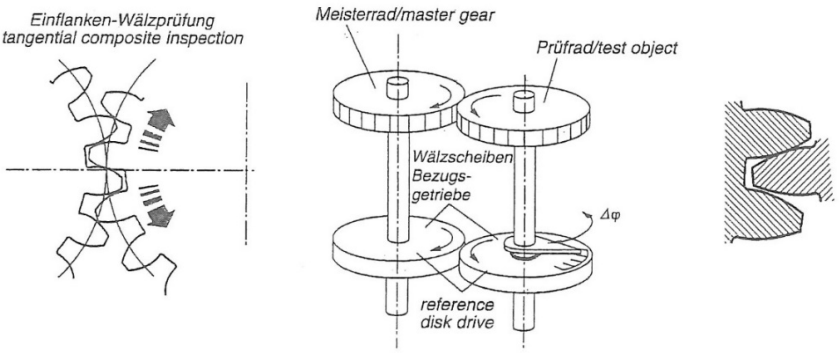

Fig. 1. Tangential composite test (source [10])

The test results are evaluated in accordance with ISO 1328-1:2013 [9] or DIN 21772:2012 [21]. They are normally expressed as a sinusoidal graph (*Fig.* 2) where the tangential composite deviation (Fi') is the difference between the maximum plus and the maximum minus angular deviation from an initial value; and the tooth-to-tooth tangential composite deviation (fi') is the greatest difference of the angular deviations of a tooth pitch. In addition, the tangential composite deviation (Fi') is divided into its long- and short-wave components, (fl') and (fk'). The standards ISO 1328-1:2013 [9] and DIN 3963:1978 [22] for cylindrical gears, DIN 3965-3:1986 [23] for bevel gears and DIN 3974-1:1975 [24] for worm gears are used to assign the corresponding tolerance grade. Variations in the gear affecting the runout, profile, pitch and accumulated pitch could be derived from the analysis of the parameter results of the test [14], [25–29].

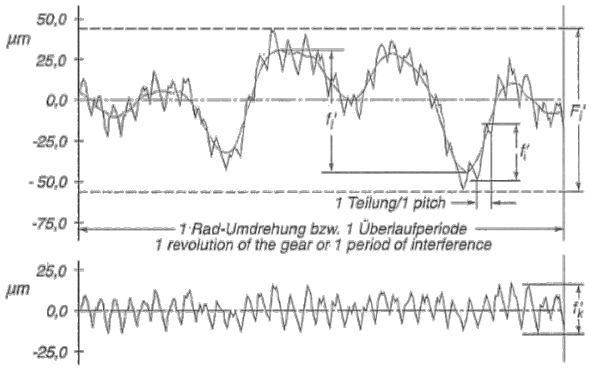

Fig. 2. Evaluation of the tangential composite inspection (source [10])

The last update of ISO 1328-1:2013 [9] includes changes in the parameters' names of the tangential composite test. In this way, *Fi'* changes to *Fis* and *fi'* is substituted by *fis*. The parameter *fl'* from VDI/VDE 2608 [10] was already named as *Fp'* in ISO 1328-1:1995 [30], terminology used in this work as it is more commonly extended in industrial and academic environments.

2.1 Description of the single-flank rolling testing machine

The single-flank rolling test machine used in this work is a retrofit of an old gear profile-measuring machine Klingelnberg PFS 600. The design of the machine follows the design guidelines established in [31], [32], the applicable standards VDI/VDE 2608 [10], AGMA 915-1-A02 [33] for tangential gear measurements and AGMA 915-2-A05 for radial gear measurement [34]. This work focuses on worm and worm gear transmissions type and therefore the criteria defined in ANSI/AGMA 2111-A98 [35] and ANSI/AGMA 2011-B14 [36] are applied. *(Fig. 3)* shows the single-flank rolling test set-up for worm and worm gear transmission types according to [35].

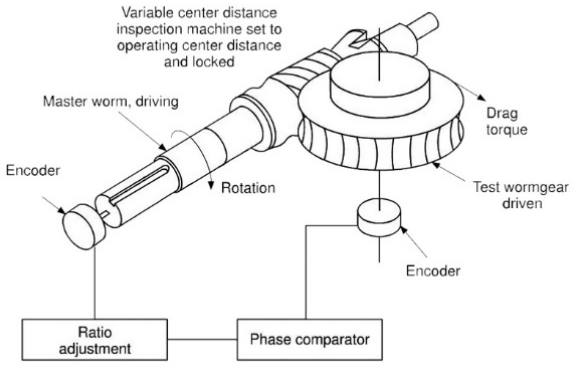

Fig. 3. Worm and worm gear tangential composite test according to ANSI/AGMA 2111-A98 (source [35]*)*

The equipment measures worm gear diameters from 100 to 600 mm and modules between 2 and 12. Therefore, the master worm maximum diameter will be 150 mm and the worm's length 1000 mm. The machine with coordinate reference system represented in *(Fig 4)* consists of a fixed mechanized steel bench (marked as 1 in Fig. 4) and a fixed worm-holder column that has a fixed position (marked 2 in Fig 4). Along this column moves the vertical carriage (z-axis) where the crosspiece is located. This configuration allows not only a height but also a worm shaft angle (y-axis) regulation. The headstock and tailstock could move along the crosspiece to adjust different worm's lengths. On the other side, the worm gear carriage (3 in Fig 4) fixes manually the gears at their nominal centre distance (x-axis) by means of a hand wheel and a spindle. Over the spindle, the machine includes a high precision shaft where the worm gear is located in the test. It includes an angular encoder and an adjustable brake, elements that are needed for the single flank rolling test configuration.

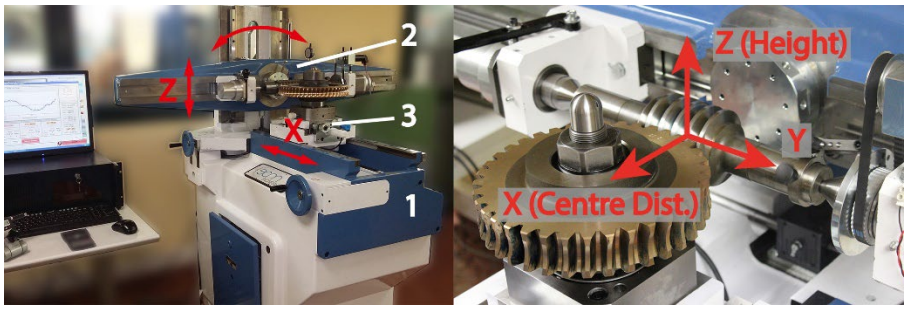

Fig. 4. Main parts of single-flank rolling test machine

Regarding the measuring instruments, the machine has two angular encoders Heidenhain RON 287 [37] for the measurement of the worm and worm gear's rotation angles with a precision of ± 2.5" for a complete revolution of the gears. The measurement of the gears' centre distance along the x-axis and the gears' relative height in the z-axis is done with two linear encoders Heidenhain LF 485 C [38]. The linear encoder precision is ± 3 µm for lengths up to 1220 mm. In addition, we included in the machine a dial gauge for the gears' axes perpendicularity measurement, reference TESA of ± 1 µm accuracy.

3 Single-flank rolling test uncertainty estimation

One of the main parameters of the tangential composite test is the tangential composite deviation (Fi') which is the difference between the maximum and minimum angular deviation between gear and worm gear in the course of one revolution or entire period (Eq. (1) and (2)).

$$F_i' = Max(\varphi_{measurement} - \varphi_{nominal}) - Min(\varphi_{measurement} - \varphi_{nominal}) = Max(\varphi_{measurement}) - Min(\varphi_{measurement}) \quad (1)$$

$$\varphi_{measurement} = \varphi_{real} + Error \quad (2)$$

Where:

$\varphi_{measurement}$ is the angular deviation between gear and worm gear in the course of one revolution;
$\varphi_{nominal}$ is the nominal variation between the worm and worm gear rotation angles, equal to zero;
φ_{real} is the real angular deviation between gear and worm gear in the course of one revolution;
Error includes the possible variations not captured by the measuring instruments;

The error associated to the *Fi'* parameter measurement could be divided according to the different steps of the tangential composite test. The uncertainty budget includes the following influences: the initial calibration of the equipment, the displacement to the nominal gears' centre distance, the height positioning, the assembling of the worm between the tail and headstock, the assembling of the worm gear in the worm gear- holder column and finally the test execution. All of them are error sources affecting the angular encoder's readings and the final measurement results.

Because there is no available standard including an uncertainty budget model for single-flank rolling tests, it is proposed in this work a specific uncertainty budget model for worm and worm gear single-flank rolling tests. The uncertainty model in Eq. (3) allows estimating the rolling testing machine's uncertainty based on the experimental calibration data and the experimental characterization of the individual parameters.

$$U_{95} = k\left[\left(u_0^2 + u_{cd}^2 + u_h^2 + u_{worm}^2 + u_{wormg}^2 + u_{sf}^2\right)^{0.5}\right] \quad (3)$$

Where:

U_{95} expanded uncertainty considering a 95% probability that the true value will be located in the calculated interval;
k coverage factor, k=2 for the 95% confidence interval considering a normal distribution of the data;
u_0 standard uncertainty due to the initial calibration of the equipment, gauges and measuring instrument's errors;
u_{cd} standard uncertainty due to the movement of the horizontal carriage from the initial calibration point to the test execution point at the gears' nominal centre distance;
u_h standard uncertainty due to the movement of the vertical carriage from the initial calibration point to test execution point at the nominal height;
u_{worm} standard uncertainty due to the assembling and driving of the worm;
u_{wormg} standard uncertainty due to the assembling and positioning of the worm gear;
u_{sf} standard uncertainty due to the single-flank rolling test execution including both angular encoders' precision and dynamic effects.

The calibration and the experimental characterization of the single-flank rolling tester were done in a metrological laboratory maintaining controlled environmental temperature (20±0.5° C) and cleaning conditions. Besides, the repeatability series have been carried out during weeks so that factors such as time, machine's stability, re-calibration of some measuring instruments and operators' influence could be considered.

To perform the test, we use a one-start master worm of 59 mm pitch diameter and a test worm gear of 281 mm pitch diameter and 55 teeth. Both gears have a pressure angle of 20°, a normal module of 5.09 and helix angle of 4.949°. The nominal centre distance of the gears is 170 mm and the height between the hub plane and the reference side of the worm gear is 45 mm. The test conditions are the following: constant angular worm speed of 25 rpm and a breaking torque of 3 Nm is applied to the worm gear's shaft.

Furthermore, the effective degrees of freedom [2] necessary to obtain the coverage factor for the expanded uncertainty were calculated according to the Welch-Satterthwaite expression (4).

$$v_{eff} = \frac{u_c^4(y)}{\sum_{i=1}^{N} \frac{u_i^4(y)}{v_i}} \quad (4)$$

Where:

v_{eff} effective degrees of freedom of $u_c(y)$;
$u_c(y)$ combined standard uncertainty of output estimate y;
$u_i(y)$ component of combined standard uncertainty $u_c(y)$ of output estimate y;
v_i degrees of freedom, of uncertainty component $u_i(y)$

The sensitivity coefficients, as partial derivatives, show the contribution of each error source to the single-flank rolling test parameters and are applied to each component of the error. Due to the complexity of the single flank rolling tests, it is necessary to assess in the uncertainty model the

contribution of each error source. In this case, the errors in the centre distance; in the relative height between hobbing planes; and in the perpendicularity between gears' axes have different effects on the rolling parameters. The values of the sensitivity coefficients were experimentally characterized. We carried out a series of different tests where we changed gradually the distance between centres (cd), the height (h) and the perpendicularity between axes (p) and we measured the difference between the maximum variations of the rolling parameter (F_i'') and their nominal positions' variations. These differences were accounted as the values for the sensitivity coefficients (c_{cdFi}), (c_{hFi}) and (c_{pFi}). It was experimentally proved that one micrometre variation in the distance between centres means 0.063 μm in the tangential composite deviation *Fi'* (c_{cdFi}). Likewise, each micrometre deviation in the height affects 0.096 μm in Fi' (c_{hFi}), and 0.046 μm is the effect in Fi' of one arc second variation in the gears' axes perpendicularity (c_{pFi}).

The breakdown of the different error's components is following explained in order to estimate the measurement uncertainty of the single-flank rolling test machine.

3.1 Uncertainty of the initial calibration (u_0)

The uncertainty due to the initial calibration (u_0) comprises multiple elements such as the uncertainty of the reference gauges used, the error of the linear encoder's readings in the calibration point, the error due to the height calibration and the error in the calibration of the angle between the gears' axes. This is a combined uncertainty calculated as the quadratic sum of all the components (5).

$$u_0^2 = u_{0cg}^2 + u_{0encx}^2 + u_{0cgz}^2 + u_{0encz}^2 + u_{0p}^2 \quad (5)$$

Where,

- u_{0cg} standard uncertainty due to the cylindrical gauges in the distance between centres calibration;
- u_{0encx} standard uncertainty due to the error of the linear encoder (x-axis);
- u_{0cgz} standard uncertainty due to the cylindrical gauge in the height calibration;
- u_{0encz} standard due to the error of the linear encoder (z-axis);
- u_{0p} standard uncertainty due to the calibration of the perpendicularity between the gears' axes.

The first uncertainty component (u_{0cg}) is calculated as the square root of the quadratic sum of the uncertainties of the cylindrical gauges used in the calibration of the rolling tester with the corresponding sensitivity coefficients in Eq. (6), which are a cylindrical gauge (u_{0cgw}) and the worm gear shaft (u_{0cgwg}). Both uncertainty expressions include the uncertainty of the coordinate measuring machine (CMM) used in the calibration process (u_{CMM}), the error of the calibration process (u_{cgw} , u_{cgwg}), and the variance due to the influence of the temperature in the gauge's dimensions (u_{tcgw} , u_{tcgwg}). The sensitivity coefficient (c_{cdFi}) was applied showing the effect of the variation in the gears' centre distance in the tangential composite deviation Fi' and we obtain the expressions (7) and (8).

$$u_{0cg}^2 = \left(\frac{1}{2}\right)^2 u_{0cgw}^2 + \left(\frac{1}{2}\right)^2 u_{0cgwg}^2 \quad (6)$$

$$u_{0cgw}^2 = u_{CMM}^2 + u_{cgw}^2 + u_{tcgw}^2 = c_{cdFi}^2 \left(\frac{U_{99\,(CMM)}}{k_{CMM}}\right)^2 + c_{cdFi}^2 \frac{s_{cgw}{}^2}{n} + c_{cdFi}^2 \frac{\left(d_{cgw} \propto_{max} \Delta t_{max}\right)^2}{3} \quad (7)$$

$$u_{0cgwg}^2 = u_{CMM}^2 + u_{cgwg}^2 + u_{tcgwg}^2 = c_{cdFi}^2 \left(\frac{U_{99\,(CMM)}}{k_{CMM}}\right)^2 + c_{cdFi}^2 \frac{s_{cgwg}{}^2}{n} + c_{cdFi}^2 \frac{\left(d_{cgwg} \propto_{max} \Delta t_{max}\right)^2}{3} \quad (8)$$

The second component (u_{0encx}) is calculated according to (9) applying the sensitivity coefficient (c_{cdFi}) to the error of the linear encoder in the measurement in the x-direction (E_{encx}). The linear encoder model and precision value are included in section 2.1.

$$u_{0encx}^2 = c_{cdFi}^2 \left(\frac{E_{encx}}{\sqrt{3}}\right)^2 \quad (9)$$

The height calibration is obtained by means of the contact between the gauge cylinder and the reference surface. Therefore, the third component (u_{0cgz}) is calculated using Eq. (7) with the corresponding sensitivity coefficient (c_{hFi}) obtaining the following expression (10):

$$u_{0cgz}^2 \left(\frac{1}{2}\right)^2 \left[c_{hFi}^2 \left(\frac{U_{99\,(CMM)}}{k_{CMM}}\right)^2 + c_{hFi}^2 \frac{{s_{cgw}}^2}{n} + c_{hFi}^2 \frac{\left(d_{cgw} \propto_{max} \Delta t_{max}\right)^2}{3}\right] \quad (10)$$

The fourth component (u_{0encz}) includes the uncertainty due to the linear encoder error (E_{encz}), with equal value to (E_{encx}), in the measurement along the z-axis to position the worm-carriage. The sensitivity coefficient to apply in this case is c_{hFi} (11).

$$u_{0encz}^2 = c_{hFi}^2 \left(\frac{E_{encz}}{\sqrt{3}}\right)^2 \quad (11)$$

Finally, the last component (u_{0p}) shows the uncertainty due to the calibration of the angle between the gears' axes measuring the perpendicularity. It includes the perpendicularity regulation error (u_{pr}) and the uncertainty of the dial gauge used in the measurement (u_{pdg}). The hysteresis of the system, 4 µm, was measured with the dial gauge and represents an error of 2.95 arc seconds in the angle between the gears' axes (H_{pr}). The dial gauge's accuracy (R_{pdg}) of 1 µm means an error of 0.7 arc seconds in the angle (E_{pdg}). Equation (12) shows the expression of (u_{0p}) with its components weighted by the effect of the perpendicularity error in the Fi' parameter (c_{pFi}).

$$u_{0p}^2 = u_{pr}^2 + u_{pdg}^2 = c_{pFi}^2 \left(\frac{H_{pr}/2}{\sqrt{3}}\right)^2 + c_{pFi}^2 \left(\frac{E_{pdg}/2}{\sqrt{3}}\right)^2 \quad (12)$$

3.2 Uncertainty of the main carriage movement to the gears' nominal centre distance (u_{cd})

The uncertainty due to the movement of the main carriage from the calibration point to the nominal distance between gears' centres position is shown in Eq. (13). In this expression, (u_{lix}) is the measuring uncertainty derived from the laser interferometer used in the calibration; (u_{encx}) is associated to the error of the linear encoder measuring along the x-axis; and (u_{cdb}) includes the errors due to the backlash between the linear guides and the main horizontal carriage.

$$u_{cd}^2 = u_{lix}^2 + u_{encx}^2 + u_{cdb}^2 \quad (13)$$

The first uncertainty component (u_{lix}) includes the error of the laser interferometer (± 0.5 ppm). The maximum travel is 400 mm, resulting in an error of ± 0.2 µm (14). The sensitivity coefficient (c_{cdFi}) was applied showing the effect of the variation in the gears' centre distance in the tangential composite deviation Fi'.

$$u_{lix}^2 = c_{cdFi}^2 \left(\frac{E_{lix}}{\sqrt{3}}\right)^2 \quad (14)$$

The second component (u_{encx}), is the uncertainty due to the precision of the linear encoder in the calibration of the final position along the x-axis (15).

$$u_{encx}^2 = c_{cdFi}^2 \left(\frac{E_{encx}}{\sqrt{3}} \right)^2 \quad (15)$$

Finally, the third component (u_{cdb}) is composed of the uncertainties of the different geometric errors during the main carriage movement along the x-axis. The uncertainty (u_{cdb}) expression is shown in Eq. (16). It comprises the uncertainty due to the residual positioning error after the numerical compensation (u_{cdc}); the uncertainty due to the straightness error in z-direction (u_{cdEZX}); the uncertainty due to the pitch error (u_{cdEBX}); and the uncertainty due to the roll error (u_{cdEAX}). Due to their different effect on the rolling parameters, we applied different sensitivity coefficients to all of them. The positioning error (E_{xx}) generates uncertainty in the distance between centres. The straightness error in z-direction and the pitch error could modify the height and the roll error affects the perpendicularity between the gears' axis.

Due to the fact that there is neither calibration nor evaluation standards for this type of equipment, we followed the scarce recommendations for double-flank rolling testers according to AGMA 2116 [19] and AGMA 935 [39] standards, as well as for gear measurement equipment stated in ISO 18653 [18] and ISO/TR 100064-5 [20]. In addition, we used common techniques used in verification and calibration of machine tools, CMMs and GMIs [40], [41], [42], ISO 230-1 [43] and ISO 230-2 [44].

To determine the errors, five bi-directional approaches (ISO 230-2 [44]) were done every 10 mm from 0 to 200 and every 25 mm from 200 to 400 mm in the distance between centres. The encoder readings were compared with those of the interferometer and the numerical compensation was applied. The positioning error was determined as the difference between the maximum and the minimum of the offset positions. Subsequently, with a similar procedure the straightness and angular errors were calculated (ISO 230-1 [43]). Finally, the error values were established, considering as the functional point the meshing point between the worm gear and the largest possible worm. In this way, the largest possible errors that included the total volume of the machine and therefore the greatest uncertainty were considered.

$$u_{cdb}^2 = u_{cdc}^2 + u_{cdEZX}^2 + u_{cdEBX}^2 + u_{cdEAX}^2 \quad (16)$$

The positioning error (E_{xx}) was assessed with a laser interferometer giving an error of 3.2 µm and it includes the uncertainties of the position, pitch and yaw errors in the movement in the x-direction. In addition, a straightness error in the z-direction (E_{ZX}) of 56 µm and a pitch error (E_{BX}) of 76 µm were assessed. A roll error (E_{AX}) of 13 arc seconds shows the angle's difference between the gears' axes in the x-direction travel. Due to the different contributions of the before mentioned errors in the Fi' parameter, the corresponding sensitivity coefficients were applied in Eq. (17).

$$u_{cdb}^2 = c_{cdFi}^2 \left(\frac{E_{XX}/2}{\sqrt{3}} \right)^2 + c_{hFi}^2 \left(\frac{E_{ZX}/2}{\sqrt{3}} \right)^2 + c_{hFi}^2 \left(\frac{E_{BX}/2}{\sqrt{3}} \right)^2 + c_{pFi}^2 \left(\frac{E_{AX}/2}{\sqrt{3}} \right)^2 \quad (17)$$

3.3 Uncertainty of the vertical carriage movement to the nominal height (u_h)

The uncertainty estimation because of the movement of the vertical carriage from the height's calibration point to the nominal position is shown in Eq. (18). (u_{liz}) is the measuring uncertainty derived from the laser interferometer used in the calibration; (u_{encz}) is associated to the

error of the linear encoder measuring along the z-axis; and (u_{hb}) includes the errors due to the backlash between the linear guides and the vertical carriage.

$$u_h^2 = u_{liz}^2 + u_{encz}^2 + u_{hb}^2 \quad (18)$$

The first component (u_{liz}) in (19) includes the error of the laser interferometer. For a maximum travel of 150 mm results in an error of ± 0.075 µm. The sensitivity coefficient (c_{hFi}) was applied showing the effect of the variation of the height in the tangential composite deviation Fi'.

$$u_{liz}^2 = c_{hFi}^2 \left(\frac{E_{liz}}{\sqrt{3}}\right)^2 \quad (19)$$

The second component (u_{encz}) in (20) is the uncertainty due to the precision of the linear encoder measuring in the z-direction in the initial calibration.

$$u_{encz}^2 = u_{0encz}^2 \quad (20)$$

Finally, the third component (u_{hb}) is divided into the uncertainty due to the residual errors in the calibration and the remaining errors contributing to the Fi' parameter with the movement in the z-axis. The uncertainty (u_{hb}) expression is shown in Eq. (21). It comprises the uncertainty due to the numerical compensation (u_{hc}); the uncertainty due to the pitch error E_{BZ} (u_{hEBZ}) generated by the optics' position in the correction; the uncertainty due to the yaw error E_{AZ} (u_{hEAZ}) because of the variation of the angle between gears' axes along the z-axis travel; and the uncertainty derived from the straightness error E_{XZ} (u_{hEXZ}).

The compensation error for the linear encoder in the z-direction (E_{hc}) is 4.3 µm and it includes the uncertainties of the position error and partially pitch and yaw errors in the z-direction. The remaining part of the pitch and yaw errors are included as extra uncertainty components. Pitch error is 9 µm in height due to the optics location and yaw error is quantified in 28 arc seconds variation in the angle between gears' axes. Applying the corresponding sensitivity coefficients, we obtain the uncertainty expression in (21).

$$u_{hb}^2 = u_{hc}^2 + u_{hEBZ}^2 + u_{hEAZ}^2 + u_{hEXZ}^2 = c_{hFi}^2 \left(\frac{E_{hc}/2}{\sqrt{3}}\right)^2 + c_{hFi}^2 \left(\frac{E_{BZ}/2}{\sqrt{3}}\right)^2 + c_{pFi}^2 \left(\frac{E_{AZ}/2}{\sqrt{3}}\right)^2 + c_{cdFi}^2 \left(\frac{E_{XZ}/2}{\sqrt{3}}\right)^2 \quad (21)$$

3.4 Uncertainty of the gears' assembling (u_{worm}) and (u_{wormg})

The repeatability of the worm and worm gear assembling was experimentally assessed. The errors consider effects such as backlash, driving and misalignment of the gears' axes because of the manipulation and fixation of the gears in the test set-up. We assessed the repeatability values by means of five repetition series of ten tests where we assembly and disassembly the worm and worm gear without changing additional operating conditions. This uncertainty estimation considers a Gaussian symmetric probability function including the maximum differences in the Fi' parameter results measured in the repeatability tests. The maximum variation for the worm (E_{worm}) was 11.5 µm meanwhile we obtained an error (E_{wormg}) of 21.9 µm for the worm gear. The sensitivity coefficient is equal to one because the repeatability results depend directly on the Fi' parameter. Therefore, the related uncertainties are expressed in (22) and (23).

$$u_{worm}^2 = \left(\frac{E_{worm}/2}{2}\right)^2 \quad (22)$$

$$u_{wormg}^2 = \left(\frac{E_{wormg}/2}{2}\right)^2 \quad (23)$$

3.5 Uncertainty of the single-flank rolling test execution (u_{sf})

The last component of the general uncertainty estimation for single-flank rolling tests includes the error sources due to the test execution itself (u_{sf}). It includes the uncertainty of the angular encoder measuring the worm rotation (u_{angw}); the uncertainty of the angular encoder measuring the worm gear rotation (u_{angwg}); and the uncertainty of the remaining parameters of the test that could affect the measurement's result (u_{sfp}) as it is shown in Eq. (24).

$$u_{sf}^2 = u_{angw}^2 + u_{angwg}^2 + u_{sfp}^2 \tag{24}$$

Both angular encoders are identical and have an error (E_{ang}) of ±2.5 arc seconds in a complete revolution. As the maximum diameters for worm and worm gear are 150 mm and 600 mm respectively, the errors to be included in the uncertainty estimation will be ±0.9 µm and ±3.6 µm. The sensitivity coefficients are equal to one because the error influence is directly applied to the Fi' parameter and therefore we obtain the following expressions (25) and (26).

$$u_{angw}^2 = \left(\frac{E_{ang}}{\sqrt{3}}\right)^2 \tag{25}$$

$$u_{angwg}^2 = \left(\frac{E_{ang}}{\sqrt{3}}\right)^2 \tag{26}$$

In the expression of the uncertainty component (u_{sfp}) we could include all the error contributions derived from the tangential composite test which have not been previously considered in the estimation (27). Possible error sources are the angular rotation speed of the gears (u_{rs}) and the breaking force (u_{bf}). A final uncertainty component (u_{others}) including any other effect detected is included in the expression.

$$u_{sfp}^2 = u_{rs}^2 + u_{bf}^2 + u_{others}^2 = 0 \tag{27}$$

It was experimentally assessed in the tangential composite test execution, that following the rotation speed and breaking force recommended values included in the standard VDI/VDE 2608 [10], no significant variations in the tangential composite parameters were observed.

4 Expanded uncertainty of the single-flank rolling tester

4.1 Expanded uncertainty of Fi' parameter

The expanded uncertainty corresponding to the tangential composite deviation (Fi') is calculated according to (3) and the results obtained are shown in Table 1 including the individual contribution in percentage to the total combined uncertainty. We calculated the degrees of freedom v_{eff} for each uncertainty component and sub-components according to Eq. (4) using a bottom-up approach.

Table 1.- Expanded uncertainty of Fi' parameter

Standard uncertainty component $u(x_i)$	Source of uncertainty	$u(x_i)$ (µm)	Degrees of freedom v_{eff}	c_i	$u_i(Fi') \equiv \lvert c_i \rvert u(x_i)$ (µm)	$\frac{u(x_i)^2}{u_c(F_i')^2}$ (%)
u_0	**Initial calibration**	0.21	2428546	1	0.21	0.09

u_{0cgw}	Cylindrical gauge worm (centre distance)	0.025	836	0.5	0.012	0
u_{CMM}	CMM error	0.333	∞	0.063	0.021	0
u_{cgw}	Cylindrical gauge worm measurement	0.063	9	0.063	0.006	0
u_{tcgw}	Temperature	0.198	∞	0.063	0.008	0
u_{0cgwg}	Cylindrical gauge worm gear (centre distance)	0.023	128	0.5	0.012	0
u_{CMM}	CMM error	0.333	∞	0.063	0.021	0
u_{cgwg}	Cylindrical gauge worm gear measurement	0.095	9	0.063	0.006	0
u_{tcgwg}	Temperature	0.126	∞	0.063	0.008	0
u_{0encx}	Linear encoder error (x)	1.732	∞	0.063	0.109	0.02
u_{0cgz}	Cylindrical gauge worm (height)	0.037	836	0.5	0.020	0
u_{CMM}	CMM error	0.333	∞	0.096	0.032	0
u_{cgw}	Cylindrical gauge worm measurement	0.063	9	0.096	0.006	0
u_{tcgw}	Temperature	0.198	∞	0.096	0.019	0
u_{0encz}	Linear encoder error (z)	1.732	∞	0.096	0.166	0.06
u_{0p}	Perpendicularity calibration	0.040	∞	1	0.040	0
u_{pr}	Perpendicularity error	0.850	∞	0.046	0.039	0
u_{pdg}	Dial gauge error	0.213	∞	0.046	0.010	0
u_{cd}	**Horizontal carriage movement**	2.62	∞	1	2.62	13.75
u_{lix}	Interferometer error	0.116	∞	0.063	0.007	0
u_{encx}	Linear encoder error (x)	1.732	∞	0.063	0.109	0,02
u_{cdb}	Centre distance backlash	2.623	∞	1	2.623	13.73
u_{cdc}	Encoder numerical compensation	0.9	∞	0.063	0.06	0.01
u_{cdEZX}	Straightness error EZX	16.2	∞	0.096	1.55	4.81
u_{cdEBX}	Pitch error EBX	21.9	∞	0.096	2.11	8.85
u_{cdEAX}	Roll error EAX	3.8	∞	0.046	0.17	0.06
u_{h}	**Vertical carriage movement**	0.49	∞	1	0.49	0.48
u_{liz}	Interferometer error	0.043	∞	0.096	0.004	0
u_{encz}	Linear encoder error (z)	1.732	∞	0.096	0.166	0.06
u_{hb}	Height backlash	0.463	∞	1	0.463	0.42
u_{hc}	Encoder numerical compensation	1.2	∞	0.096	0.119	0.02
u_{hEBZ}	Pitch error EBZ	2.6	∞	0.096	0.249	0.12
u_{hEAZ}	Yaw error EAZ	8.1	∞	0.046	0.372	0.28
u_{hEXZ}	Straightness error EXZ	0	∞	0.063	0	0
u_{worm}	**Worm assembling**	2.88	∞	1	2.88	16.50
u_{wormg}	**Worm gear assembling**	5.48	∞	1	5.48	59.83
u_{sf}	**Single-flank rolling test execution**	2.16	∞	1	2.16	9.35
u_{angw}	Angular encoder error (worm)	0.53	∞	1	0.53	0.55
u_{angwg}	Angular encoder error (worm gear)	2.1	∞	1	2.1	8.80
u_{sfp}	Single flank test parameters	0	-	1	0	0
u_{rs}	Rotation speed	0	-	1	0	0
u_{bf}	Breaking force	0	-	1	0	0
u_{others}	Others	0	-	1	0	0
	$u_c^2(F_i') = \sum u_i^2(F_i') = u_0^2 + u_{cd}^2 + +u_h^2 + u_{worm}^2 + u_{wormg}^2 + u_{sf}^2$ $= 50.09\ \mu m^2$ **Combined standard Uncertainty** $7.08\ \mu m$				$u_c(F_i') =$ $v_{eff}(F_i') = 3x10^{12}$	
	Expanded Uncertainty				$U_{Fi'}(k=2) = 14.2\ \mu m$	

Taking into account the results obtained, the expanded uncertainty value is ±14.2 µm, being the worm gear assembling the most influencing contribution with a percentage of 59.83%. Other representative contributions covering the 40% of the estimated expanded uncertainty are the movement of the main carriage until the nominal centre distance, the worm's assembling and the single-flank rolling test execution. This uncertainty value is calculated for the complete working volume of the rolling tester because we considered the maximum pitch diameters for worm and worm gear.

Reducing the working volume of the tester to the usual working area, and considering the gears' pitch diameters commonly used, we obtained an expanded uncertainty value of the machine shown in Table 2. In this case, we considered a movement in the main carriage for the worm from 100 to 200 mm and a travel from 30 to 50 mm in the vertical carriage for the worm gear. The pitch diameters considered for the angular encoders' uncertainty calculation were 100 mm for the worm and 400 mm for the worm gear.

Table 2.- Expanded uncertainty of Fi' parameter in reduced tester's working area

Standard uncertainty component u(x_i)	**Source of uncertainty**	$u(x_i)$ **(µm)**	**Degrees of freedom** v_{eff}	$\frac{u(x_i)^2}{u_c(F_i')^2}$ **(%)**
u_0	Initial calibration	0.21	2428546	0.10
u_{cd}	Horizontal carriage movement	1.29	∞	3.97
u_h	Vertical carriage movement	0.20	∞	0.09
u_{worm}	Worm assembling	2.88	∞	19.64
u_{wormg}	Worm gear assembling	5.48	∞	71.24
u_{sf}	Single-flank rolling test execution	1.44	∞	4.95
$u_c^2(F_i') = \sum u_i^2(F_i') = u_0^2 + u_{cd}^2 + u_h^2 + u_{worm}^2 + u_{wormg}^2 + u_{sf}^2 = 42.08\ \mu m^2$ **Combined standard Uncertainty**			$u_c(F_i') = 6.49\ \mu m$ $v_{eff}(F_i') = 2x10^{12}$	
Expanded Uncertainty			$U_{Fi'}(k=2) = 13.0\ \mu m$	

The uncertainty estimation in the reduced working area of the tester minimized 8.4 % the uncertainty value given in Table 1. The contribution of the different sources of uncertainty to the Fi' parameter are the same than in the complete working volume of the machine. The main error source is the assembling of the worm gear. Therefore, an improvement in the fixing of the worm gear will have a clear influence in the reduction of the measurement uncertainty in the single-flank rolling tester.

4.2 Expanded uncertainty of other single-flank rolling test parameters.

The tooth- to-tooth tangential composite deviation (*fi'*) and the long-wave component of the tangential composite deviation (*Fp'*) uncertainties could be equally obtained to *Fi'* uncertainty according to expression (3). For that purpose, we will need the suitable sensitivity coefficients and their corresponding repeatability values in the gear's assembling.

Table 3 shows the expanded uncertainty calculation for the long-wave component of the tangential composite deviation (*Fp'*) for the complete working volume. The sensitivity coefficients calculated in former work of the authors that have been used for the *Fp'* parameter were c_{cdFp} = 0.024, c_{hFp} = 0.056 and c_{pFp} = 0.036. The errors due to the worm and worm gear assembling were 8.5 µm and 23.2 µm respectively. With these data, the expanded uncertainty value obtained slightly diminishes. The main error sources are the worm gear and worm assembling and the single-flank rolling test execution.

Table 3.- Expanded uncertainty of Fp' parameter

Standard uncertainty component u(xi)	**Source of uncertainty**	$u(x_i)$ **(µm)**	**Degrees of freedom** v_{eff}	$\frac{u(x_i)^2}{u_c(F_p')^2}$ **(%)**
$\mathbf{u_0}$	Initial calibration	0.11	5120326	0.03
$\mathbf{u_{cd}}$	Horizontal carriage movement	1.53	∞	5.18
$\mathbf{u_h}$	Vertical carriage movement	0.35	∞	0.26
$\mathbf{u_{worm}}$	Worm assembling	2.13	∞	9.96
$\mathbf{u_{wormg}}$	Worm gear assembling	5.80	∞	74.23
$\mathbf{u_{sf}}$	Single-flank rolling test execution	2.16	∞	10.33
$u_c^2(F_p') = \sum u_i^2(F_p') = u_0^2 + u_{cd}^2 + u_h^2 + u_{worm}^2 + u_{wormg}^2 + u_{sf}^2 = 45.32\ \mu m^2$ **Combined standard Uncertainty** $u_c(F_p') = 6.73\ \mu m$ $v_{eff}(F_p') = 6x10^{13}$				
Expanded Uncertainty $U_{Fp'}(k=2) = 13.5\ \mu m$				

In addition, Table 4 shows the expanded uncertainty calculation for the tooth-to-tooth tangential composite deviation (*fi'*) for the complete working volume. The errors due to the worm and worm gear assembling were 2.6 µm and 4.4 µm according to previous data. These value are lower than in the other parameters *(Fi', Fp')* because initially they should not be affected by the assembling's eccentricity. As a result, the uncertainty components are also reduced. The sensitivity coefficients applied to the *fi'* parameter were c_{cdfi} = 0.147, c_{hfi} = 0.258 y c_{pfi} = 0.097. It is remarkable that these coefficients are higher than the others mentioned in this work are. This is due to the fact that *fi'* parameter is particularly sensitive to any error in the following variables: distance between gears' centres, height between gears and perpendicularity between gears' axes. The uncertainty estimation supports this assumption, mainly in the component related to the main carriage movement, which has greatly increased because of the straightness and pitch errors. In fact, the expanded uncertainty of *fi'* parameter is higher than the estimations for *Fi'* and *Fp'* parameters when it should decrease, at least proportional to the measurement range required.

Table 4.-Expanded uncertainty of fi' parameter

Standard uncertainty component u(xi)	**Source of uncertainty**	$u(x_i)$ **(µm)**	**Degrees of freedom** v_{eff}	$\frac{u(x_i)^2}{u_c(f_i')^2}$ **(%)**
$\mathbf{u_0}$	Initial calibration	0.53	3067193	0.49
$\mathbf{u_{cd}}$	Horizontal carriage movement	7.05	∞	86.18

u_h	Vertical carriage movement	1.17	∞	2.37
u_{worm}	Worm assembling	0.65	∞	0.73
u_{wormg}	Worm gear assembling	1.10	∞	2.10
u_{sf}	Single-flank rolling test execution	2.16	∞	8.13

$$u_c^2(f_i') = \sum u_i^2(f_i') = u_0^2 + u_{cd}^2 + u_h^2 + u_{worm}^2 + u_{wormg}^2 + u_{sf}^2 = 57.62\ \mu m^2$$

Combined standard Uncertainty $u_c(f_i') = 7.6\ \mu m$

$v_{eff}(f_i') = 1x10^{11}$

Expanded Uncertainty $U_{fi'}(k=2) = 15.2\ \mu m$

5 Uncertainty budget optimization

As we concluded before, the worm gear assembling is the major error contribution to the uncertainty estimation. In fact, due to its big value it is not possible to know precisely the other components' influence in the total uncertainty. Based on that, this section proposes a new uncertainty estimation approach. It considers the most common gear sizes used in the industry (maximum diameters of 100 mm for the worm and 400 mm for the worm gear), the usual working area of the rolling tester (travels were limited to 200 mm for the distance between centres and to 50 mm for the height), and also tries to minimize the effect of the gears' clamping. In this way, it is possible to deepen in the influence analysis of the other error sources. Assuming that the improvement of the clamping system would eliminate the eccentricity, we have considered the same repeatability values of the worm and worm gear assembling for *Fi'* and *Fp'* as for the *fi'* parameter, which is supposed to be eccentricity-free. In addition, for the optimization of the uncertainty of fi' parameter, the experimental repeatability of this parameter proves that evaluating only a part of the angle, one tooth and not a complete revolution, the error of the angular encoder in the worm gear shaft could be estimated in ± 0.5 arc seconds. This assumption could not be applied to the uncertainty of the worm rotation since it rotates one complete revolution per worm gear's tooth.

As it is shown in Table 5 and Table 6, under these new assumptions, the expanded uncertainty of the *Fi'* parameter diminishes 67% and 50% in the case of the *fi'* parameter in comparison to the values obtained in Table 2 and Table 4. In the case of *Fi'*, the expanded uncertainty value obtained, 4.7 µm, could be considered as acceptable. Nevertheless, the *fi'* expanded uncertainty is still high, 7.6 µm, mainly due to the effect of the sensitivity coefficients that amplify the effects of the individual contributions. The *Fp'* new expanded uncertainty value, 4.1 µm, is reduced a 69%, following the same behaviour as the Fi' parameter.

Table 5.- Optimized expanded uncertainty of Fi' parameter

Standard uncertainty component $u(x_i)$	Source of uncertainty	$u(x_i)$ (µm)	c_i	$u_i(Fi') \equiv \lvert c_i \rvert u(x_i)$ (µm)	$\frac{u(x_i)^2}{u_c(F_i')^2}$ (%)
u_0	**Initial calibration**	**0.21**	**1**	**0.21**	**0.79**
u_{cd}	**Horizontal carriage movement**	**1.29**	**1**	**1.29**	**30.58**
u_{lix}	Interferometer error	0.12	0.063	0.007	0.00

https://doi.org/10.1016/j.measurement.2019.107051

u_{encx}	Linear encoder error	1.73	0.063	0.109	0.22
u_{cdb}	Centre distance backlash	1.29	1	1.29	30.36
u_{cdc}	Encoder numerical compensation	0.87	0.063	0.06	0.05
u_{cdEZX}	Straightness error EZX	4.88	0.096	0.47	4.01
u_{cdEBX}	Pitch error EBX	12.41	0.096	1.19	25.97
u_{cdEAX}	Roll error EAX	2.89	0.046	0.13	0.32
u_h	**Vertical carriage movement**	**0.20**	**1**	**0.20**	**0.72**
u_{worm}	**Worm assembling**	**0.65**	**1**	**0.65**	**7.73**
u_{wormg}	**Worm gear assembling**	**1.10**	**1**	**1.10**	**22.13**
u_{sf}	**Single-flank rolling test execution**	**1.44**	**1**	**1.44**	**38.06**
u_{angw}	Angular encoder error (worm)	0.35	1	0.35	2.24
u_{angwg}	Angular encoder error (worm gear)	1.40	1	1.40	35.82
u_{sf}	Others	0	1	0	0.00
$u_c^2(F_i') = \sum u_i^2(F_i') = u_0^2 + u_{cd}^2 + u_h^2 + u_{worm}^2 + u_{wormg}^2 + u_{sf}^2 = 5.47\ \mu m^2$					
Combined standard Uncertainty				$u_c(F_i') = 2.34\ \mu m$	
Expanded Uncertainty				$U_{Fi'}(k=2) = 4.7\ \mu m$	

Table 6.- Optimized expanded uncertainty of fi' parameter

Standard uncertainty component $u(x_i)$	Source of uncertainty	$u(x_i)$ (µm)	c_i	$u_i(f_i') \equiv \lvert c_i \rvert u(x_i)$ (µm)	$\frac{u(x_i)^2}{u_c(f_i')^2}$ (%)
u_0	**Initial calibration**	**0.53**	**1**	**0.53**	**1.97**
u_{cd}	**Horizontal carriage movement**	**3.46**	**1**	**3.46**	**83.39**
u_{lix}	Interferometer error	0.12	0.147	0.02	0.00
u_{encx}	Linear encoder error	1.732	0.147	0.25	0.45
u_{cdb}	Centre distance backlash	3.45	1	3.45	82.94
u_{cdc}	Encoder numerical compensation	0.87	0.147	0.13	0.11
u_{cdEZX}	Straightness error EZX	4.88	0.258	1.26	11.01
u_{cdEBX}	Pitch error EBX	12.41	0.258	3.20	71.21
u_{cdEAX}	Roll error EAX	2.89	0.097	0.28	0.54
u_h	**Vertical carriage movement**	**0.52**	**1**	**0.52**	**1.90**
u_{worm}	**Worm assembling**	**0.65**	**1**	**0.65**	**2.94**
u_{wormg}	**Worm gear assembling**	**1.10**	**1**	**1.10**	**8.41**
u_{sf}	**Single-flank rolling test execution**	**0.45**	**1**	**0.45**	**1.40**
u_{angw}	Angular encoder error (worm)	0.35	1	0.35	0.85
u_{angwg}	Angular encoder error (worm gear)	0.28	1	0.28	0.54
u_{sf}	Others	0	1	0	0.00
$u_c^2(f_i') = \sum u_i^2(f_i') = u_0^2 + u_{cd}^2 + u_h^2 + u_{worm}^2 + u_{wormg}^2 + u_{sf}^2 = 14.39\ \mu m^2$					
Combined standard Uncertainty				$u_c(f_i') = 3.79\ \mu m$	

Expanded Uncertainty	$U_{fi'}(k=2)=7.6\ \mu m$

In this point and based on the uncertainty components' contribution in percentage to the rolling parameters' uncertainty shown in the last columns of Tables 5 and 6, one solution to keep minimizing the uncertainty in the single-flank rolling tests would be adjusting the assembling of the horizontal worm gear carriage's linear guides to diminish both pitch (E_{BX}) and straightness error (E_{ZX}). Likewise, the use of higher precision angular encoders would help to eliminate partially the former errors, improving as a result the uncertainty values of the *Fi'* and *Fp'* parameters. Table 7 shows a summary of the expanded uncertainty values of the *Fi', fi'* and *Fp'* parameters before and after the optimization together with their variation in percentage.

Table 7.-Expanded uncertainties of (Fi', Fp', fi',) before and after optimization

	F_i' (µm)	F_p' (µm)	f_i' (µm)
U	14.2	13.5	15.2
U_{opt}	4.7	4.2	7.6
Variation (%)	67%	69%	50%

The gear's accuracy grade depends on the gear diameter and its normal module. In our case we measured a 281 mm diameter and 5.09 mm normal module worm gear, as we stated in section 3. Considering the uncertainty values obtained for the Fi', Fp' and fi' parameters shown in Table 7 and the single-flank parameter values according to ISO1328-1 standard, we consider that we could measure with the single-flank rolling tester described in this work, worm gears with accuracy grade 6 if we focus on the Fi' and Fp'. But considering the uncertainty value obtained for the fi', we could measure accuracy grade 9 worm gears. Therefore it would be needed to implement specific actions in the uncertainty sources contributing to the fi' parameter so that its uncertainty value could be improved.

6 Conclusions

As formerly explained in this paper, to assure compatibility among different gear-rolling testers it is necessary to estimate the uncertainty of the measuring process. For the time being, there has not been identified any methodology for uncertainty estimation of single flank rolling tests. Moreover, the majority of the standards focus on double flank rolling tests for gears with parallel axes. The first conclusion of the work is that the uncertainty estimation according to ANSI/AGMA 2116-05 [19] is scarcely adaptable to single-flank rolling tests for gears with non-parallel axes. Therefore, we developed a complete uncertainty budget expression for worm and worm gear single-flank rolling testers including the most representative error sources and their individual contribution's degree to the uncertainty.

The main advantage of splitting the uncertainty into individual components is that their individual contribution can be characterized. In this way, it is possible to raise corrections to minimize the error values improving the complete accuracy of the rolling measuring process. In the case study presented in this work, the results of the uncertainty budget show that it is important to guarantee an eccentricity-free assembling of the gears. The initial calibration of the gears' distance between centres and relative height is not as critical as expected, despite most test set-ups focus on

this fact. Another important factor to reduce the uncertainty of the single-flank rolling tester is the backlash between the linear guides and carriages. It was also validated that pitch and straightness errors modify the rolling test results. In addition, the study proves that the tooth- to-tooth tangential composite deviation (*fi'*) is the tangential composite parameter that shows the highest sensitivity to the error sources. Therefore, we would need to implement new corrective actions to diminish the uncertainty of fi' parameter to analogue values of the Fi' and Fp' parameters.

After developing and analysing the generic uncertainty budget expression for single-flank rolling tests for worm and worm gears, we propose an uncertainty optimization considering the usual reduced tester working volume, common gears' diameters and minimizing the clamping effect of the gears. The uncertainty model presented links not only with the measurement equipment but also with the calibration procedure and the test execution. We could identify with this model the individual error sources contributions in the test and the behaviour of the different components of a gear-rolling tester. Finally, it is important to point out that despite we carried out the uncertainty budget analysis for single-flank rolling testers with perpendicular gears' axes, it could be also applied to other type of gears and configurations.

7 References

[1] Joint Committee for Guides in Metrology, JCGM 200:2012. International vocabulary of metrology – Basic and general concepts and associated terms (VIM), (2012).

[2] Joint Committee for Guides in Metrology, JCGM 100:2008 Evaluation of measurement data: Guide to the expression of uncertainty in measurement (GUM 1995 with minor corrections), (2008). doi:10.1373/clinchem.2003.030528.

[3] E. Lawson, The basics of gear metrology and terminology. I. Gear Technology (USA), 1998.

[4] E. Lawson, The basics of gear metrology and terminology part II. Gear Technology (USA), 15 (6) (1998) 67–71.

[5] G. Goch, Gear Metrology, CIRP Ann. 52 (2003) 659–695. doi:10.1016/S0007-8506(07)60209-1.

[6] M.A. Corporation., Gear Inspection, Gear Technol. 30 (1) (2013) 11–3.

[7] D. Gimpert, An elementary guide to gear inspection., Gear Solut. 32 (2005) 8.

[8] ISO 1328-2:1997 Cylindrical gears - ISO system of accuracy - Part 2: Definitions and allowable values of deviations relevant to radial composite deviations and runout information, (1997).

[9] ISO 1328-1:2013 Cylindrical gears - ISO system of accuracy - Part 1: Definitions and allowable values of deviations relevant to corresponding flanks of gear teeth, (2013).

[10] VDI/VDE 2608 Tangential composite and radial composite inspection of cylindrical gears, bevel gears, worm and worm wheels, (2001).

[11] J. Tang, J. Jia, Z. Fang, Z. Shi, Development of a gear measuring device using DFRP method, Precis. Eng. 45 (2016) 153–159. doi:10.1016/J.PRECISIONENG.2016.02.006.

[12] J. Tang, Y. Zhang, Z. Shi, Radial and tangential error analysis of double-flank gear measurement, Precis. Eng. 51 (2018) 552–563. doi:10.1016/J.PRECISIONENG.2017.10.011.

[13] F. Zheng, X. Guo, M. Zhang, Non-uniform flank rolling measurement for shaped noncircular gears, Measurement. 116 (2018) 207–215. doi:10.1016/J.MEASUREMENT.2017.07.048.

[14] M. Pueo, J. Santolaria, R. Acero, A. Gracia, A review of tangential composite and radial composite gear inspection, Precis. Eng. 50 (2017) 522–537. doi:10.1016/j.precisioneng.2017.05.007.

[15] R.C. Frazer, Measurement uncertainty in gear metrology, Newcastle University, 2007.

[16] E. Reiter, F. Eberle, Practical Considerations for the Use of Double-Flank Testing for the Manufacturing Control of Gearing - Part I, Gear Technol. 31 (2014) 44–51. http://www.geartechnology.com/articles/0114/Practical_Considerations_for_the_Use_of_D

ouble-Flank_Testing_for_the_Manufacturing_Control_of_Gearing_-_Part_I.
[17] E. Reiter, F. Eberle, Practical Considerations for the Use of Double-Flank Testing for the Manufacturing Control of Gearing - Part II, Gear Technol. 31 (2014) 60–69. http://www.geartechnology.com/articles/0314/Practical_Considerations_for_the_Use_of_Double-Flank_Testing_for_the_Manufacturing_Control_of_Gearing_-_Part_II.
[18] ISO 18653:2003 Gears - Evaluation of instruments for the measurement of individual gears, (2003).
[19] ANSI/AGMA 2116-A05 Evaluation of Double Flank Testers for Radial Composite Measurement of Gears, (2005).
[20] ISO/TR 10064-5:2005 Code of inspection practice - Part 5: Recommendations relative to evaluation of gear measuring instruments, (2005).
[21] DIN 21772:2012 Gears – cylindrical involute gears and gear pairs – definition of deviations., (2012).
[22] DIN 3963:1978 Tolerances for cylindrical gear teeth – tolerances for working deviations., (1978).
[23] DIN 3965-3:1986 Tolerancing of bevel gears; tolerances for tangential composite errors., (1986).
[24] DIN 3974-1:1995 Accuracy of worms and worm gears – Part 1: General bases., (1995).
[25] R.E. Smith, The relationship of measured gear noise to measured gear transmission errors. AGMA Technical Paper, (87FTM6)., AGMA. (1987).
[26] R.E. Smith, Solving gear noise prob with single flank inspection., Power Transm. Des. (1990) 63–7.
[27] R.E. Smith, Identification of gear noise with single flank composite measurement. AGMA Technical Paper, (85FTM13)., AGMA. (1985).
[28] R.E. Smith, What single flank measurement can do for you. AGMA Technical Paper (84FTM2), AGMA. (1984).
[29] R.G. Munro, Effect of Geometrical Errors on the Transmission of Motion between Gears, Proc. Inst. Mech. Eng. 184 (15) (1969) 79–84.
[30] ISO, ISO 1328-1:1995 Cylindrical gears - ISO system of accuracy - Part 1: Definitions and allowable values of deviations relevant to corresponding flanks of gear teeth, (1995).
[31] P. Schellekens, N. Rosielle, H. Vermeulen, M. Vermeulen, S. Wetzels, W. Pril, Design for Precision: Current Status and Trends, CIRP Ann. 47 (1998) 557–586. doi:10.1016/S0007-8506(07)63243-0.
[32] Bewoor. A., V.A. Kulkarni, Metrology and measurement, Tata McGraw-Hill Educ. (2009).
[33] AGMA 915-1, AGMA 915-1-A02 Inspection Practices - Part 1: Cylindrical Gears - Tangential Measurements, (2002).
[34] AGMA 915-2, AGMA 915-2-A05 Inspection Practices - Part 2: Cylindrical Gears - Radial Measurements, (2005).
[35] ANSI/AGMA 2011-A98 Cylindrical Wormgearing Tolerance and Inspection Methods, (1998).
[36] ANSI/AGMA 2011-B14 Cylindrical Wormgearing Tolerance and Inspection Methods, (2014).
[37] Heidenhain, “Angle Encoders - With integral bearing.,” 2013.
[38] Heidenhain, “Linear Encoders - For numerically controlled machine tools.,” 2014.
[39] AGMA 935-A05, AGMA 935-A05 Recommendations Relative to the Evaluation of Radial Composite Gear Double Flank Testers, (2005).
[40] H. Schwenke, W. Knapp, H. Haitjema, a. Weckenmann, R. Schmitt, F. Delbressine, Geometric error measurement and compensation of machines-An update, CIRP Ann. - Manuf. Technol. 57 (2008) 660–675. doi:10.1016/j.cirp.2008.09.008.
[41] R.C. Frazer, J. Hu, Methods of testing calibration equipment in the UK’s national gear metrology laboratory, in: D.G.P. Ford SR (Ed.), Laser Metrol. Meachine Perform. III, 1997: pp. 231–241. http://library.witpress.com/pages/PaperInfo.asp?PaperID=7969.
[42] R. Bicker, R.C. Frazer, D. Wehrneyer, Verifying position errors in CNC gear measuring instruments using a laser interferometer with dynamic data capture software, in: Laser

Metrol. Mach. Perform. V, 2001: pp. 345–354.

[43] ISO 230-1:2012 Test code for machine tools - Part 1: Geometric accuracy of machines operating under no-load or quasi-static conditions., (2012).

[44] ISO 230-2:2014 Test code for machine tools - Part 2: Determination of accuracy and repeatability of positioning of numerically controlled axes., (2014).